ORIGINAL ARTICLE

CrossMark

Metabolomics Study of Immune Responses of New Zealand Greenshell™ Mussels (*Perna canaliculus*) Infected with Pathogenic *Vibrio* sp.

Thao V. Nguyen[1] · Andrea C. Alfaro[1] · Tim Young[1] · Sridevi Ravi[1] · Fabrice Merien[2]

Abstract

Vibrio coralliilyticus is a bacterial pathogen which can affect a range of marine organisms, such as corals, fish and shellfish, with sometimes devastating consequences. However, little is known about the mechanisms involved in the host-pathogen interaction, especially within molluscan models. We applied gas chromatography-mass spectrometry (GC-MS)-based metabolomics to characterize the physiological responses in haemolymph of New Zealand Greenshell™ mussels (*Perna canaliculus*) injected with *Vibrio* sp. DO1 (*V. coralliilyticus/neptunius*-like isolate). Univariate data analyses of metabolite profiles in *Vibrio*-exposed mussels revealed significant changes in 22 metabolites at 6 h post-infection, compared to non-exposed mussels. Among them, 10 metabolites were up-regulated, while 12 metabolites were down-regulated in infected mussels. Multivariate analyses showed a clear distinction between infected and non-infected mussels. In addition, secondary pathway analyses indicated perturbations of the host innate immune system following infection, including oxidative stress, inflammation and disruption of the TCA cycle, change in amino acid metabolism and protein synthesis. These findings provide new insights into the pathogenic mechanisms of *Vibrio* infection of mussels and demonstrate our ability to detect detailed and rapid host responses from haemolymph samples using a metabolomics approach.

Keywords Mussel immunology · Metabolite profiles · Bacterial infection · Host-pathogen interactions · Shellfish health · Flow cytometry · Haemolymph

Introduction

Bacteria in the genus *Vibrio* (e.g. *V. aestuarianus*, *V. tubiashii*, *V. coralliilyticus*, *V. tapetis*, *V. spendidus* and *V. harveyi*) have been associated with a number of infectious diseases in marine bivalves (reviewed by Travers et al. 2015). Among them, infections with *V. coralliilyticus* have been reported in several marine organisms. This bacterium is a well-known coral

pathogen that causes tissue lysis of *Pocillopora damicornis* in the Indian Ocean and Red Sea (Ben-Haim et al. 2003; Rozenblat and Rosenberg 2004). Recently, it has been shown to cause mortality in a number of fish and shellfish species (Austin et al. 2005; Genard et al. 2013). *V. coralliilyticus* is a gram-negative, motile and facultative anaerobic bacterium (Plumb and Hanson 2011), which is phylogenetically related to *V. tubiashii* (Ben-Haim et al. 2003). Therefore, many marine isolates of *V. coralliilyticus* from shellfish were misidentified as *V. tubiashii* until recently when the genomes of several *V. coralliilyticus* strains have been sequenced (Kehlet-Delgado et al. 2017; Richards et al. 2014). Therefore, previous emergences of *V. tubiashii* in bivalve shellfish aquaculture on the west coast of North America (Brown 1981; Dumbauld et al. 2011; Elston et al. 1981; Elston et al. 2008) were possibly caused by *V. coralliilyticus* (Richards et al. 2015). In previous work, pathogen challenges with *V. coralliilyticus* induced significant larval mortality in New Zealand green-lipped mussels (*P. canaliculus*) (Kesarcodi-Watson et al. 2009a, b), great scallops (*Pecten maximus*), European flat oysters (*Ostrea edulis*) (Kesarcodi-

✉ Andrea C. Alfaro
andrea.alfaro@aut.ac.nz

1 Aquaculture Biotechnology Research Group, School of Science, Faculty of Health and Environmental Sciences, Auckland University of Technology, Private Bag 92006, Auckland 1142, New Zealand

2 AUT-Roche Diagnostics Laboratory, School of Science, Faculty of Health and Environmental Sciences, Auckland University of Technology, Private Bag 92006, Auckland 1142, New Zealand

Watson et al. 2012), Eastern oysters (*Crassostrea virginica*) and Pacific oysters (*Crassostrea gigas*) (Richards et al. 2015). These suggest that *V. coralliilyticus* is an important pathogen for bivalves that has contributed to dramatic losses in shellfish aquaculture worldwide in recent years. Despite the fact that *V. coralliilyticus* appear to be a global bivalve pathogen, there is limited information about its pathogenicity, infection mechanism and/or disease mitigation.

As filter feeders, bivalves are always exposed to pathogen-rich environments, and mostly rely on an innate immune system with non-specific defense mechanisms composed of cellular and humoral components (Song et al. 2010). Cellular components include haemocytes and epithelial cells, whereas humoral components include various active molecules secreted by haemocytes and released into the haemolymph (Allam and Raftos 2015; Song et al. 2010). Haemocytes are considered to be the backbone of the bivalve immune system and they play major roles in phagocytosis, encapsulation and nacrezation of invading pathogens and parasites (Allam and Raftos 2015; Anderson and Good 1976; Song et al. 2010). These specialized cells are also involved in other biological functions, such as wound healing, food digestion, transport of nutrients, gonad resorption, shell formation and secretion of humoral factors (Allam and Raftos 2015; Bachère et al. 2015). Despite a recent proliferation of cellular and molecular studies focusing on bivalve immunology (Allam and Raftos 2015; Bachère et al. 2015), immune response to pathogenic infections of bivalves is not fully understood (Bassim et al. 2015; Estes et al. 2004; Yue et al. 2013). Part of the reason for this lack of understanding may be that current immunological and molecular biology techniques are still not sufficiently advanced to clearly elucidate the complex mechanisms of infections within a host-pathogen model.

'Omics' is an encompassing term for relatively new approaches to the study of large sets of biological molecules and comprises genomics, transcriptomics, proteomics and metabolomics (Smith et al. 2005). The advancement of high-throughput technologies and rapid development of bioinformatics have led to an expansion of omics applications in a variety of life science fields (Alfaro and Young 2016; Gómez-Chiarri et al. 2015; Guo and Ford 2016). Amongst these omics, transcriptomics (the study of the transcriptome or group of mRNA molecules present in a biological system) has been widely used in many areas of aquaculture research, such as selective breeding, stress physiology and toxicology, developmental biology, disease resistance and immunology (reviewed by Li and Li 2014). In bivalve immunity studies, high-throughput transcriptomics has been used for finding the immune-related genes/transcripts or pathways in oysters (Fleury et al. 2009; Rosa et al. 2012; Zhang et al. 2014), mussels (Moreira et al. 2014; Philipp et al. 2012; Venier et al. 2009), clams (Hasanuzzaman et al. 2017; Milan et al. 2011; Moreira et al. 2012) and scallops (Pauletto et al. 2014; Sun et al. 2014;

Zhang et al. 2017). Compared to transcriptomics, metabolomics (study of broad sets of small molecules or metabolites present in cells, tissues, bodyfluids and entire organisms) is relatively new and its application in aquaculture research is limited (Alfaro and Young 2016; Young and Alfaro 2016). However, since metabolites are the end-products of cellular regulatory processes and are highly sensitive to environmental change, metabolomics can represent a better picture of what is actually happening in the organism at a given time (Alfaro and Young 2016). Due to its strong predictive power of phenotypes, metabolomics may provide a novel tool for understanding endogenous metabolic changes caused by many diseases across a range of host-pathogen interactions. Furthermore, metabolomics approaches can be used in early diagnosis of diseases, leading to the development of therapies and health monitoring systems.

In the present study, we report on the application of GC-MS-based metabolomics approach integrated with flow cytometry to characterize the metabolic and immunological responses in haemolymph of New Zealand Greenshell™ mussels (*Perna canaliculus*) following infection with *V. corallyliticus*-like isolate. This is an innovative metabolomics-based study of non-lethally collected haemolymph as the target sample to investigate the interaction between a bivalve host and a marine pathogen. The knowledge acquired from this study leads to a better understanding of *V. coralliilyticus* pathogenicity and future development of disease management strategies in aquaculture production.

Materials and Methods

Animal Preparation and Bacterial Culture

Adult mussels were obtained from Westpac Mussels Distributors Ltd. (Auckland, New Zealand) and acclimatized for 1 week in a re-circulation system (fresh 5 μm filtered seawater [FFSW]; temperature = 16 ± 0.5 °C; salinity = 34 ppt; pH = 8.26). Only male mussels were used in this experiment to avoid potential variations due to gender-specific responses, as previously reported for other species (Liu et al. 2014b; Lu et al. 2017). A pool of 20 mussels were selected (mean weight = 75.96 ± 10.29 g; mean shell length = 10.24 ± 0.62 cm) and randomly divided into two equal groups and placed into 50 L rectangular plastic tanks filled with continuously aerated FFSW.

The bacterial strain *Vibrio* sp. DO1 (*V. coralliilyticus*/ *neptunius*-like isolate, 99.5% 16S rDNA sequence similarity with *V. corallyliticus*, Genbank: EU358784), which was previously isolated by Kesarcodi-Watson et al. (2009a), was provided by Cawthron Institute (Nelson, New Zealand). Bacterial suspensions were prepared following the method described by

Kesarcodi-Watson et al. (2009b) with modifications. Briefly, the bacterial isolates, which were stored at −80 °C in 50% glycerol, were revived by thawing for 1 h prior to incubation in 10 mL volumes of sterilized Marine Broth 2216 (MB, Difco) at room temperature for 12 h on a G10 Gyrotory shaker (New Brunswick Scientific Co., Edison, NJ, USA) at 100 rpm. The bacterial suspension was streaked on Thiosulfate Citrate Bile Salts Sucrose (TCBS) agar plates (Fort Richard Laboratories, Auckland, New Zealand) and subcultured three times to ensure purity. Bacterial colonies were cultured in 10 mL MB for 12 h, then transferred into 500 mL MB and incubated for 36 h at room temperature on a G10 Gyrotory shaker at 100 rpm. The final broth cultures were centrifuged on an Eppendorf Centrifuge 5810 R (Eppendorf AG, Hamburg, Germany) at $2423 \times g$ for 10 min and washed twice in autoclaved phosphate-buffered saline (PBS) (137 mM NaCl, 2.7 mM KCl, 10 mM Na_2HPO_4, 2 mM KH_2PO_4, pH 7.4). The bacterial suspension was re-suspended in autoclaved PBS to the original concentration ($\sim 10^8$ CFU mL^{-1}). A series of 10-fold dilutions in PBS was prepared and measured on a spectrophotometer (Ultrospec 2100 pro UV–Vis, Biochrom Ltd., Cambridge, UK) at 600 nm to determine the cell concentration of final broth cultures. In addition, 100 μL from each dilution was spread on TCBS agar plates to verify experimental concentrations.

Challenge Experiment

Ten mussels were injected with 50 μL of Vibrio sp. DO1 suspension (10^7 cells/mL) into the adductor muscle. This concentration of bacteria was used based on results from a pilot study to stimulate the metabolic responses of mussels to the infection. The ten remaining mussels (control group) were injected with 50 μL of PBS only. After injection, all animals were put back into their respective tanks. After 6 h post-injection, approximately 1 mL of haemolymph was collected from each animal by gently inserting a needle (25 gauge and 5/8″ needle) attached to a 3 mL sterile syringe (Terumo, Japan) into the posterior adductor muscle. Immediately after withdrawal, samples were transferred into 2 mL Eppendorf tubes and kept on ice. Haemolymph of 300 μL was subsequently pipetted into 2 mL Cryovials (BioStor™), immediately flash-frozen in liquid nitrogen and stored at −80 °C until metabolite analyses were carried out. The remaining haemolymph was stored briefly (ca. 30 min) on ice for bacterial counts and flow cytometry assays.

Bacterial Quantification

Selective isolation and quantification of Vibrio sp. in the haemolymph were performed using the spread plate method with a turntable and glass spreader, according to Sanders (2012). Briefly, 100 μL of haemolymph from each mussel in the control group was directly spread on TCBS agar plates (Fort Richard Laboratories, Auckland, New Zealand). For infected mussels, 1:10 serial dilutions (up to 10^{-4}) in PBS were prepared from neat haemolymph samples and 100 μL from each dilution was similarly plated. All plates were incubated at room temperature for 24 h. Then, colony forming units (cfu) were enumerated; where cfu/mL = (no. of colonies x dilution factor)/volume of each sample.

Flow Cytometric Analyses

Sub-samples of the remaining haemolymph were used to assess total cell count, haemocyte viability and production of intracellular reactive oxygen species (ROS) via flow cytometry using a Muse® Cell Analyzer (EMD Millipore, Hayward, CA, USA). Haemocyte concentration and viability parameters were measured for each sample using the Muse® Cell Count and Viability Kit (EMD Millipore) following the manufacturer's specifications, as previously described by Grandiosa et al. (2016). Relative quantification of ROS was estimated using the Muse® Oxidative Stress kit (EMD Millipore) that simultaneously determines the count and percentage of cells producing ROS based on the intracellular detection of superoxide radicals using dihydroethidium staining (Bindokas et al. 1996). Haemolymph samples from infected and control mussel groups were diluted in 1× assay buffer at an optimal concentration of 1×10^6 haemocytes per mL, mixed with the Muse® Oxidative Stress working solution (1:20 dilution) and incubated for 30 min at 37 °C according to the manufacturer's specifications.

GC-MS-Based Metabolomics

Metabolites from haemolymph samples of both mussel groups were co-extracted with an internal standard (L-alanine-2,3,3,3-d$_4$) in cold methanol-water solution (MeOH:H$_2$O), according to Villas-Bôas et al. (2011) with minor modifications. Briefly, 300 μL of mussel haemolymph was slowly thawed on ice and mixed with 20 μL of d4-alanine (10 mM) prior to drying on a SpeedVac Concentrator with a Refrigerated Vapor trap (Savant™ SC250EXP, Thermo Scientific) for 4 h (0 °C, vacuum level 3). Dried samples were extracted with 500 μL of cold (−20 °C) 50% MeOH:H$_2$O solution and 500 μL of cold 80% MeOH:H$_2$O. The mixture was vortexed vigorously for 1 min, re-frozen on dry ice then thawed again. Extracts were cold (−6 °C) centrifuged at 2500 rpm for 10 min (Centrifuge 5810 R, Eppendorf AG, Hamburg, Germany), and supernatants from both extractions were collected in 2 mL plastic vials placed on dried ice and dried in the SpeedVac concentrator specified above.

Extracted metabolites were derivatized via methyl chloroformate (MCF) alkylation, following Villas-Bôas et al. (2011), with minor modifications. Briefly, dried samples were

re-suspended in 400 μL of 1 M sodium hydroxide and quantitatively transferred to Kimble™ silanized borosilicate glass tubes (12 × 75 mm) (ThermoFisher, Auckland, New Zealand) containing 334 μL of methanol and 68 μL of pyridine. MCF reagent of 40 μL (Sigma-Aldrich, St. Louis, MO, USA) was added and the mixture was vortexed for 30 s. Another 40 μL of MCF was added, followed by vortexing for 30 s. To separate the MCF derivatives from the mixture, 400 μL of chloroform (Merck, Darmstadt, Germany) was added, vortexed for 10 s, then followed by addition of 800 μL of 50 mM sodium bicarbonate (Merck, Darmstadt, Germany) solution and vortexed for a further 10 s. The mixture was centrifuged at 2500 rpm on an Eppendorf Centrifuge 5810 R (Eppendorf AG, Hamburg, Germany) for 6 min. The upper aqueous layer was discarded and a small amount of anhydrous sodium sulphate (BDH Chemicals, Poole, UK) was added to remove residual H_2O. The chloroform phase containing the MCF derivatives was transferred to 2 mL amber CG glass vials fitted with inserts (Sigma-Aldrich, St. Louis, MO, USA). A sample blank containing 20 μL of L-alanine-2,3,3,3-d4 was similarly derivatized for quality control (QC) purposes, along with a separate standard amino acid mix (100 μL, 20 mM [Merk, Darmstadt, Germany]).

Immediately after derivatization, the MCF derivatives were injected into a GC-MS system (Agilent GC7890B coupled to a MSD5977A with a Agilent autosampler [Agilent Technologies, USA], with a quadrupole mass selective detector [EI] operated at 70 eV). The system was equipped with a ZB-1701 GC capillary column (30 m × 250 μm id × 0.15 μm with 5-m stationary phase [86% dimethylpolysiloxane, 14% cyanopropylphenyl]) (Phenomenex, Torrance, CA, USA). The instrumental setup parameters were conducted according to Smart et al. (2010). Samples (1 μL) were injected under pulsed splitless mode with the injector temperature at 260 °C. The helium gas flow through the GC-column was set at a constant flow of 1 mL min^{-1}. The GC-oven temperature was initially held at 45 °C for 2 min, and then raised with a gradient of 9 °C min^{-1} to 180 °C. After 5 min, the temperature was increased at 40 °C min^{-1} to 220 °C. After a further 5 min, the temperature was increased at 40 °C min^{-1} to 240 °C and held for 11.5 min. Finally, the temperature was increased at 40 °C min^{-1} until it reached 280 °C, where it was held for a further 2 min. The interface temperature was set to 250 °C, the source was set at 230 °C and the quadrupole temperature was set at 150 °C. The mass spectrometer was operated in scan mode (starting after 6 min; mass range 38–650 amu at 1.47 scans sec^{-1}). Identification of compounds was carried out using mass spectra acquired in scan mode from 38 to 550 amu, with detection threshold of 100 ion counts. A derivatized sample blank containing the internal standard, a derivatized standard amino acid mix, a non-derivatized standard alkane mix and a sample of pure chloroform solvent were also injected and analyzed for QC purposes.

Spectral Processing

Deconvolution and identification of GC-MS data were performed using AMDIS (Automated Mass Spectral Deconvolution and Identification System) software (version 2.66) from NIST (National Institute of Standards and Technology, USA). Subsequently, R (version 3.3.1) and in-house MassOmics package (The University of Auckland) were used to produce a summary report and to integrate peaks. Peak height data were manually checked with ChemStation software (Agilent Technologies) for the presence of contaminants. Repeats (based on ID number, match factor and retention time) and aberrant records were removed.

Statistical Analyses

Metabolite data were normalized to the peak intensity of the internal standard (D4-alanine) to compensate for potential technical variations (e.g. variable metabolite recoveries), glog transformed and mean centred prior to statistical analysis using MetaboAnalyst 3.0 software (Xia et al. 2015). Univariate analyses were performed to identify metabolite differences between infected and control groups, including Student's t test, significance analysis of microarrays/metabolites (SAM) and empirical Bayesian analysis of microarrays/metabolites (EBAM). Multivariate data analyses included the following: unsupervised principal components analysis (PCA) and hierarchical cluster analysis (HCA) (Euclidian distance; Ward's criterion) were used to identify natural groupings of samples based on the underlying structure of the data, and supervised projection to latent structure discriminant analysis (PLS-DA) was applied to minimize the possible contribution of intergroup variability and to identify discriminating features between control and infected groups. The PLS-DA model performance was validated using Leave One Out Cross Validation (LOOCV), which was assessed via accuracy, multiple correlation coefficient (R^2) and cross-validated R^2 (Q^2). The important classifiers were identified via their variable importance in projection (VIP) scores.

Quantitative enrichment analysis (QEA) (Xia and Wishart 2010) and network topology analysis (NTA) (Nikiforova and Willmitzer 2007) were performed to investigate functional relationships among the annotated metabolites for pathway analyses. Pathways involving two or more annotated metabolites that matched with the Kyoto Encyclopedia of Genes and Genomes database (Kanehisa and Goto 2000) with simultaneous QEA p-values < 0.05, QEA false discovery rates (FDRs) < 0.1 and with NTA pathway impact (PI) scores > 0.1 were considered as potential primary pathways of interest, as previously described by Young et al. (2017).

Bacterial count and flow cytometric data were analyzed with independent Student's t tests using SPSS® software (version 23.0) (IBM, Armonk, NY, USA).

Results

Bacterial Cell Counts

Vibrio counts were significantly higher (t test; $p < 0.05$) in haemolymph from infected mussels (ca. 3.22×10^5 cfu/mL), compared to those of non-infected (control) mussels (ca. 278.33 cfu/mL) (Fig. 1a).

Haemolymph Cell Counts and Viability

Haemocyte cell concentrations in haemolymph of infected and non-infected mussels were similar (ca. 4.14×10^6 cells/mL) (Fig. 1b). However, the proportion of haemocytes which were viable in haemolymph of infected mussels were substantially lower (ca. 18%) than in non-infected mussels (ca. 64%) (t test; $p < 0.05$) (Fig. 1c).

ROS Analyses

At 6 h post-injection, the number of haemocytes generating ROS were significantly ($p < 0.05$) higher in mussels injected with *Vibrio* sp. DO1 ($8.53 \pm 2.36\%$) compared to control mussels injected with PBS only ($3.01 \pm 1.25\%$) (Fig. 1d).

Metabolite Profiles

We reliably annotated 71 metabolites across broad chemical classes from the haemolymph spectra (e.g. amino acids, organic acids, fatty acids, sterols, tripeptides, vitamins).

Univariate Data Analysis

Univariate statistical analyses showed a number of differences in the metabolite profiles between infected and non-infected mussels. Firstly, t test analysis identified 24 metabolites as being significantly different between infected and non-infected mussels ($p < 0.05$). Similarly, SAM and EBAM revealed an alternation of 23 metabolites that were differentially expressed between infected and non-infected mussels (Table S1 in Supplementary materials). With a fold-change cut-off threshold of 2, we identified 22 common metabolites that were significantly different between two treatment groups. Among them, 10 metabolites were up-regulated, while 12 metabolites were down-regulated in infected mussels (Fig. 2).

Multivariate Data Analyses

Multivariate analyses of the haemolymph metabolite profiles showed good separations between infected and non-infected

Fig. 1 Flow cytometric analyses of bacterial and mussel haemolymph. **a** $\mathrm{Log_{10}}$ bacterial cell count on TCBS agar plates. **b** $\mathrm{Log_{10}}$ haemocyte counts. **c** Viability of mussel haemocytes (%). **d** Percentage of ROS (+) cells (cells exhibiting ROS) in the haemolymph. Significant differences relative to the control are marked with an asterisk (*) (Student's t test, $p < 0.05$). Error bars represent standard deviations
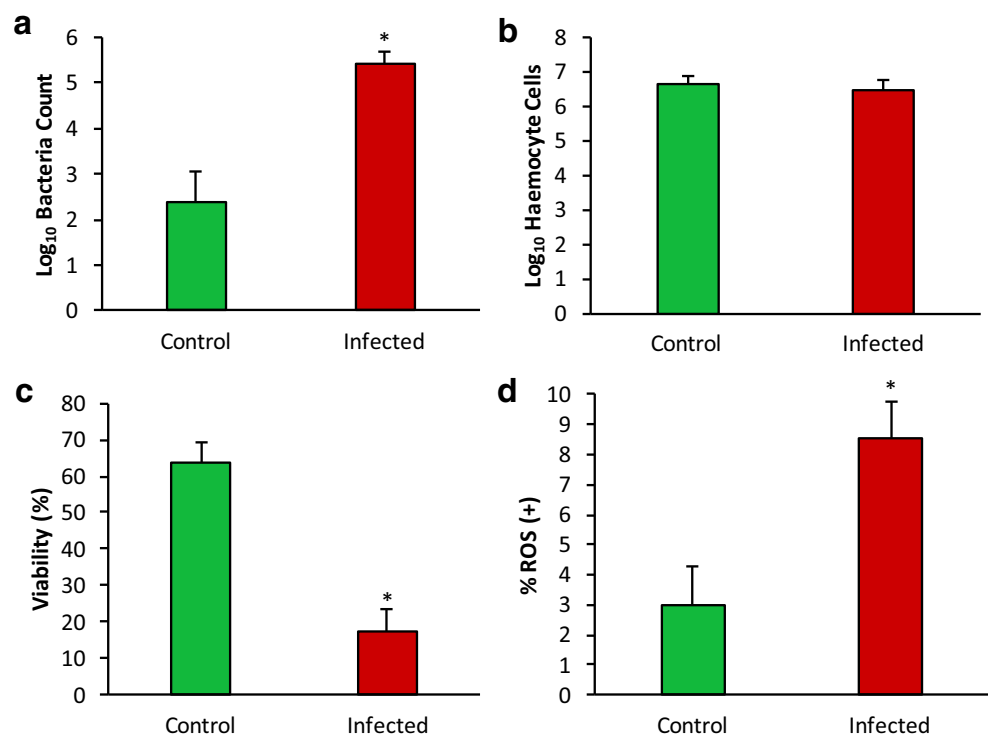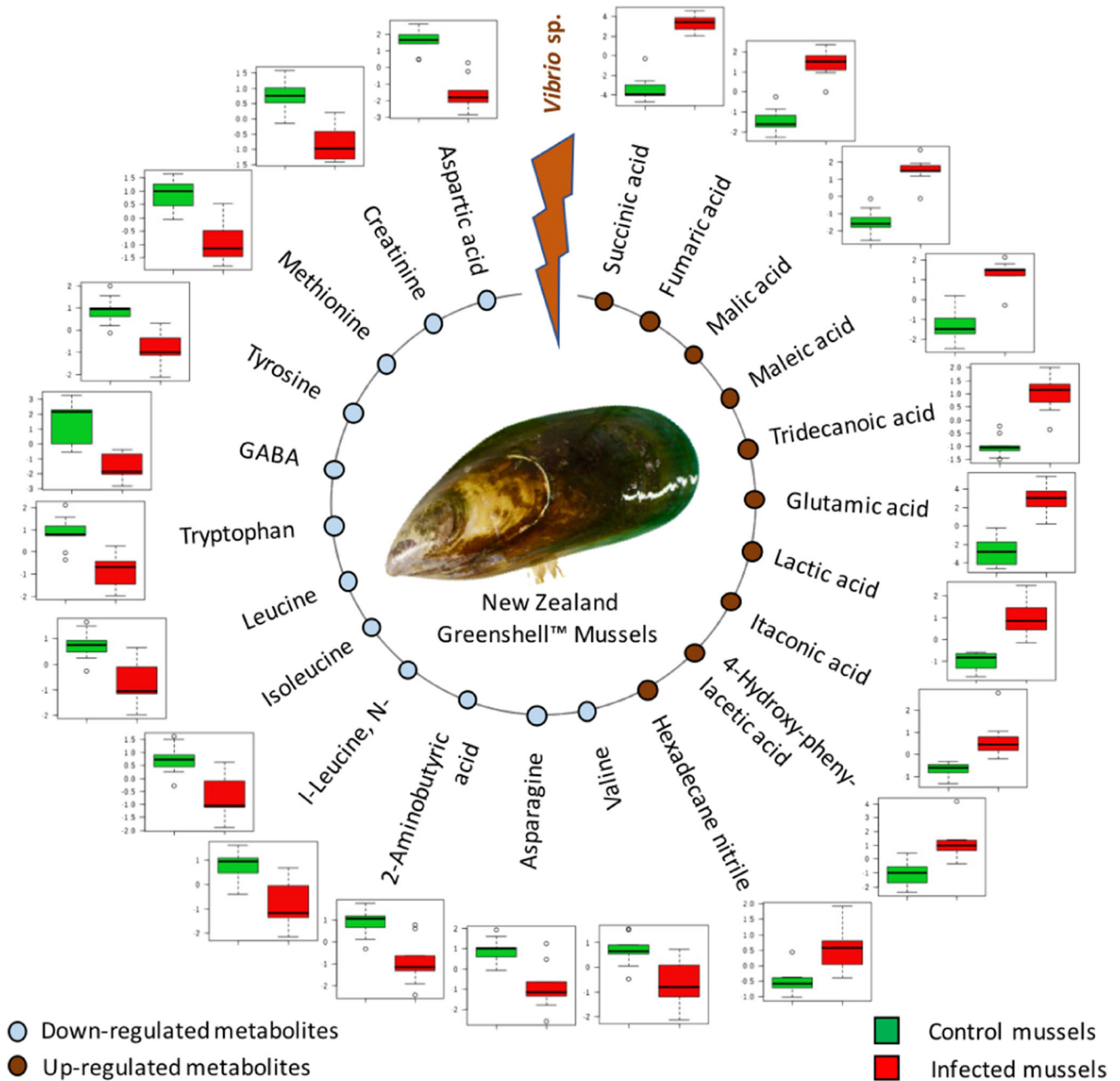
Fig. 2 Alternations of metabolites in *Vibrio* sp. infected and non-infected mussels at 6 h post-infection. Box plots of metabolites are based on *t* test analysis, showing relative abundances of metabolites in control (green) and infected mussels (red) (l-Leucine, N-: l-Leucine, N-methoxycarbonyl-, methyl ester)

mussels (Fig. 3). PCA correctly grouped the samples by their class labels, with the distribution of non-infected mussels (green dots) being clearly separated from that of infected mussels (red triangles) along the PC1 axis (Fig. 3a). These sample groupings were independently supported via unsupervised HCA (Fig. 3b), with the dendrogram revealing two clear discriminative clusters based on the treatment that they received. Supervised PLS-DA analysis sharpened the discrimination between control and infected groups (Fig. 3c). The PLS-DA model showed an accuracy of 100%, a multiple correlation

coefficient (R^2) of 95.6% and a cross-validated predictive ability (Q^2) of 92.3%. These parameters indicate optimal fitness and prediction performance of the PLS-DA model. Fifteen metabolites with VIP scores > 1.0 were identified as contributing strongly to the model (Fig. 3d).

Pathway Analysis

Pathway topology analysis showed 44 biochemical pathways that matched the KEGG database. Among these, 15
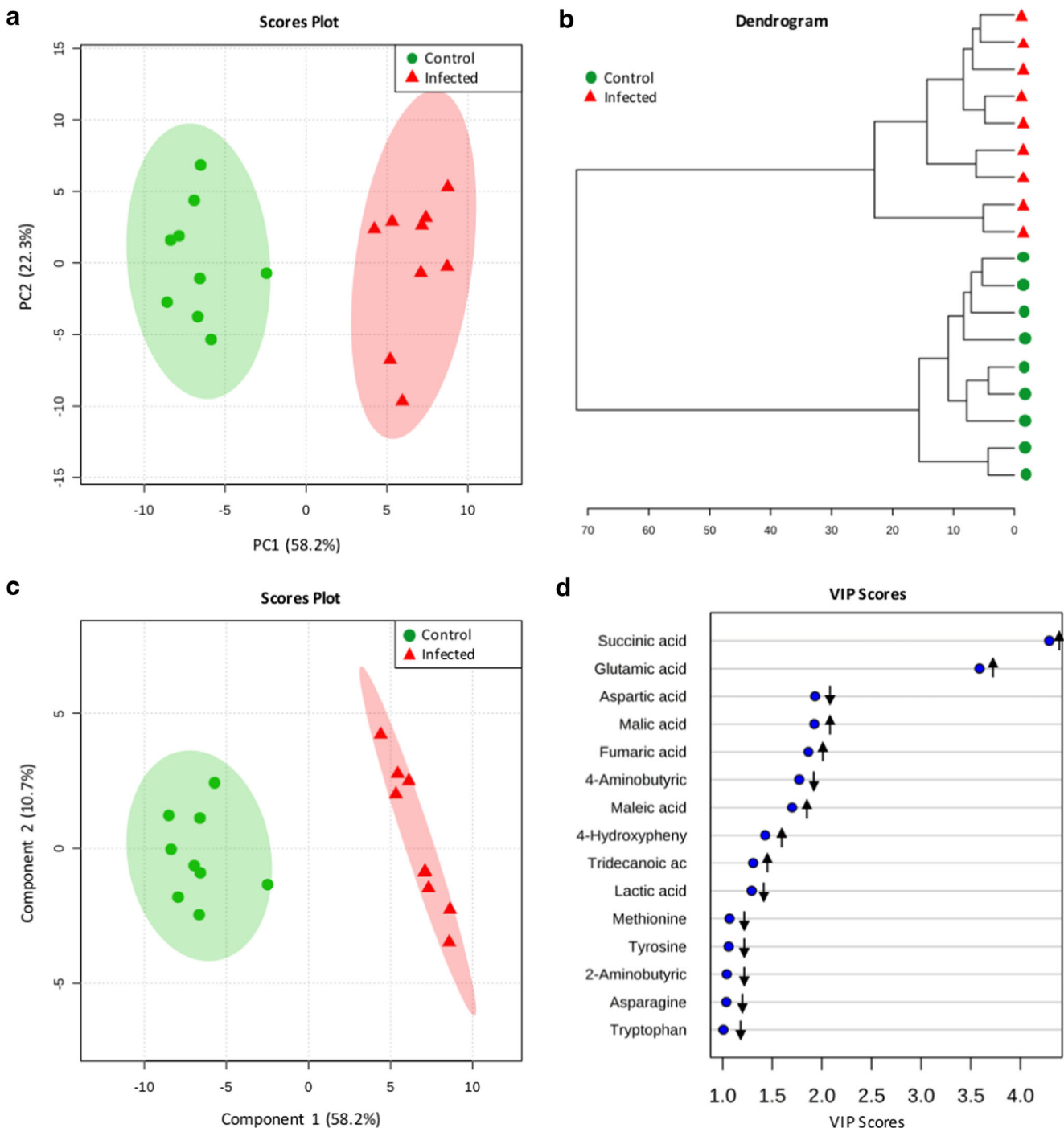
a

b

c

d

Fig. 3 Multivariate cluster analyses of metabolite profiles of *Vibrio* sp. infected and non-infected (control) mussels. **a** 2D principal component analysis (PCA) score plot. **b** Dendrogram (Euclidian distance; Ward's method). **c** 2D projection to latent structure discriminant analysis (PLS-DA) score plot. **d** Top 15 metabolites with variable importance in projection (VIP) scores for the PLS-DA model. Up and down arrows, respectively, demonstrate increased and decreased metabolites in infected mussels compared to non-infected mussels

pathways involving at least two annotated metabolites with QEA p values < 0.05, QEA FDR values < 0.1 and NTA pathway impact (PI) values > 0.1 were screened as potential primary target pathways of interest relating to the treatment effect (Table 1).

Discussion

Recent NMR-based metabolomics studies have shown changes in metabolites underlying several metabolic pathways in different bivalve organs, such as hepatopancreas and gills of

Table 1 List of altered metabolic pathways that identified as primary target pathways in mussel haemolymph during *Vibrio* sp. DO1 infection

Pathways: detected metabolites	Hits/total compounds	Raw p	-LOG(p)	FDR	Impact
Alanine, aspartate and glutamate metabolism: aspartic acid, alanine, glutamic acid, gamma-aminobutyric acid, glutamine, asparagine, fumaric acid, succinic acid.	8/24	0.000	23.456	0.000	0.719
Arginine and proline metabolism: glutamine, ornithine, aspartic acid, glutamic acid, proline, gamma-aminobutyric acid, fumaric acid.	7/43	0.000	22.919	0.000	0.322
Citrate cycle (TCA cycle): succinic acid, malic acid, citric acid, fumaric acid.	4/20	0.000	19.214	0.000	0.151
Tyrosine metabolism: Tyrosine, fumatic acid, p-Hydroxyphenylacetic acid.	3/44	0.000	18.906	0.000	0.137
Histidine metabolism: Glutamic acid, histidine, aspartic acid.	3/14	0.000	18.176	0.000	0.238
Aminoacyl-tRNA biosynthesis: asparagine, histidine, phenylalanine, glutamine, cysteine, glycine, aspartic acid, serine, methionine, valine, alanine, lysine, isoleucine, leucine, threonine, tryptophan, tyrosine, proline, glutamic acid.	19/67	0.000	17.265	0.000	0.103
Glyoxylate and dicarboxylate metabolism: citric acid, malic acid.	2/18	0.000	15.184	0.000	0.296
D-Glutamine and D-glutamate metabolism: glutamic acid, glutamine	2/5	0.000	13.846	0.000	1.000
Glutathione metabolism: glutathione, glycine, cysteine, glutamic acid, ornithine, pyroglutamic acid.	6/26	0.000	13.414	0.000	0.418
beta-Alanine metabolism: beta-alanine, aspartic acid.	2/16	0.000	11.437	0.000	0.395
Phenylalanine, tyrosine and tryptophan biosynthesis: phenylalanine, tyrosine.	2/4	0.001	7.551	0.001	1.000
Phenylalanine metabolism: phenylalanine, tyrosine.	2/11	0.001	7.551	0.001	0.407
Valine, leucine and isoleucine biosynthesis: valine, leucine and isoleucine.	4/13	0.003	5.874	0.005	1.000
Cysteine and methionine metabolism: cystathionine, serine, methionine, cysteine.	4/29	0.008	4.883	0.014	0.443

individuals infected with pathogenic *Vibrio* species (Liu et al. 2013a, b, 2014a, b). However, metabolic alterations in the host's haemolymph during *Vibrio* infections have until now been elusive. Using a GC-MS platform, we observed many metabolic responses reflected in the haemolymph of mussels 6 h post-infection with *Vibrio* sp. DO1. In infected mussels, these metabolic changes included up-regulation of 10 metabolites and down-regulation of 12 metabolites. These endogenous metabolites are important signatures of metabolic pathways and mechanisms (e.g. oxidative stress, inflammation, disruptions of TCA cycle, amino acid metabolism and protein synthesis) that are relevant to the innate immune response of mussels when infected with *Vibrio* sp. DO1.

Oxidative Stress

ROS are a natural by-product of different biological processes and have important role in protective mechanism of most organisms (Jabs 1999; Torreilles et al. 1996). However, excess of ROS production due to changes of intra- and extra-cellular environmental conditions that leads to an imbalance between ROS and antioxidants in favour of ROS can cause oxidative stress and long-term damage to cells and tissues via degradation of DNA, proteins and lipids (Jabs 1999; Torreilles et al. 1996). In this study, we observed a significantly higher percentage of ROS-producing cells in infected mussels compared to non-

infected mussels, demonstrating that *P. canaliculus* haemocytes up-regulated ROS production in response to *Vibrio* sp. DO1 infection. In agreement with this finding, previous studies have also reported increases in ROS within haemolymph samples of several other marine bivalves in response to pathogenic bacteria or stimulation of pathogen-associated molecular patterns (PAMPs) (Buggé et al. 2007; Costa et al. 2009; Goedken and De Guise 2004; Lambert et al. 2003).

In addition to the flow cytometry assay, metabolomic analyses also revealed some important metabolite signatures of potential oxidative stress in infected mussels, including altered glutathione metabolism and transsulfuration pathway (cysteine and methionine metabolism), decreased free methionine content and increased levels of glutamic and succinic acids. Glutathione in reduced form (GSH) is an important and abundant antioxidant molecule, which can react with electrophilic oxidants (e.g. H_2O_2) by converting two GSH molecules into oxidized form (GSSG) (Fig. 4) (Espinosa-Diez et al. 2015). The GSH/GSSG ratio is thus often considered to be a biomarker for oxidative stress in various physiological and pathophysiological situations (Asensi et al. 1999; Gurer-Orhan et al. 2004; Jones 2002; Zitka et al. 2012). In the present study, we identified total glutathione (GSH and GSSG) which was not different between infected mussels and control mussels, but we could not discriminate between GSH and GSSG due to the technical limitations of the GC-MS approach, so the GSH/

GSSG ratio was not obtained. However, we identified six metabolites (glutathione, glycine, cysteine, glutamic acid, ornithine and pyroglutamic acid) within the glutathione metabolic pathway, and secondary pathway analysis screened glutathione metabolism as an affected target pathway of interest relating to the treatment effect ($p = 0.000$, FDR $= 0.000$, PI $= 0.418$) (Table 1). The transsulfuration pathway is a source of cysteine for GSH synthesis under low-mid stress conditions (McBean 2012) and was also identified as a differentially regulated pathway ($p = 0.008$, FDR $= 0.014$, PI $= 0.443$). During transsulfuration, methionine acts as a precursor for homocysteine, which combines with serine to form cysteine through a cystathionine intermediate. Cysteine in turn combines with glutamic acid and then glycine to form GSH (Fig. 4) (McBean 2012). Hence, the decrease in methionine in infected mussels may suggest a high demand of methionine for the transsulfuration and glutathione pathways. The elevated levels of glutamic acid (precursor of GSH) in infected mussel haemolymph could affect GSH synthesis. Increases of intracellular glutamic acid have been reported to decrease GSH levels and eventually trigger ROS production in Riluzole-treated cells (Seol et al. 2016). These combined results may indirectly suggest the involvement of GSH in regulating elevated ROS production in haemolymph of *Vibrio*-infected mussels.

Succinic acid is an intermediate of TCA cycle, but also plays an important role in several other metabolic pathways, including the formation and elimination of ROS (reviewed by Tretter et al. 2016). Succinic acid has been shown to drive reverse electron transport (RET) and generate ROS production by RET during ischemia-reperfusion injury (Chouchani et al. 2014). Recently, Mills et al. (2016) found that increased succinate-driven oxidation by succinate dehydrogenase (SDH) and an elevated mitochondrial membrane potential combine to drive mitochondrial ROS production. In this study, we observed an increase of both ROS and succinic acid, which may suggest the significant contribution of succinic acid towards a greater production of mitochondrial ROS in infected mussels. The flow cytometry and metabolomics results herein suggest that *P. canaliculus* haemocytes are capable of producing ROS in response to *Vibrio* infection and that may lead to oxidative stress in infected mussels.

Tricarboxylic Acid Cycle (TCA Cycle)

The TCA cycle is a key metabolic pathway in all aerobic organisms that generate energy through oxidation of fuel molecules (e.g. glucose, fatty acids and certain amino acids) into carbon dioxide. Interruption of the TCA cycle in mammalian
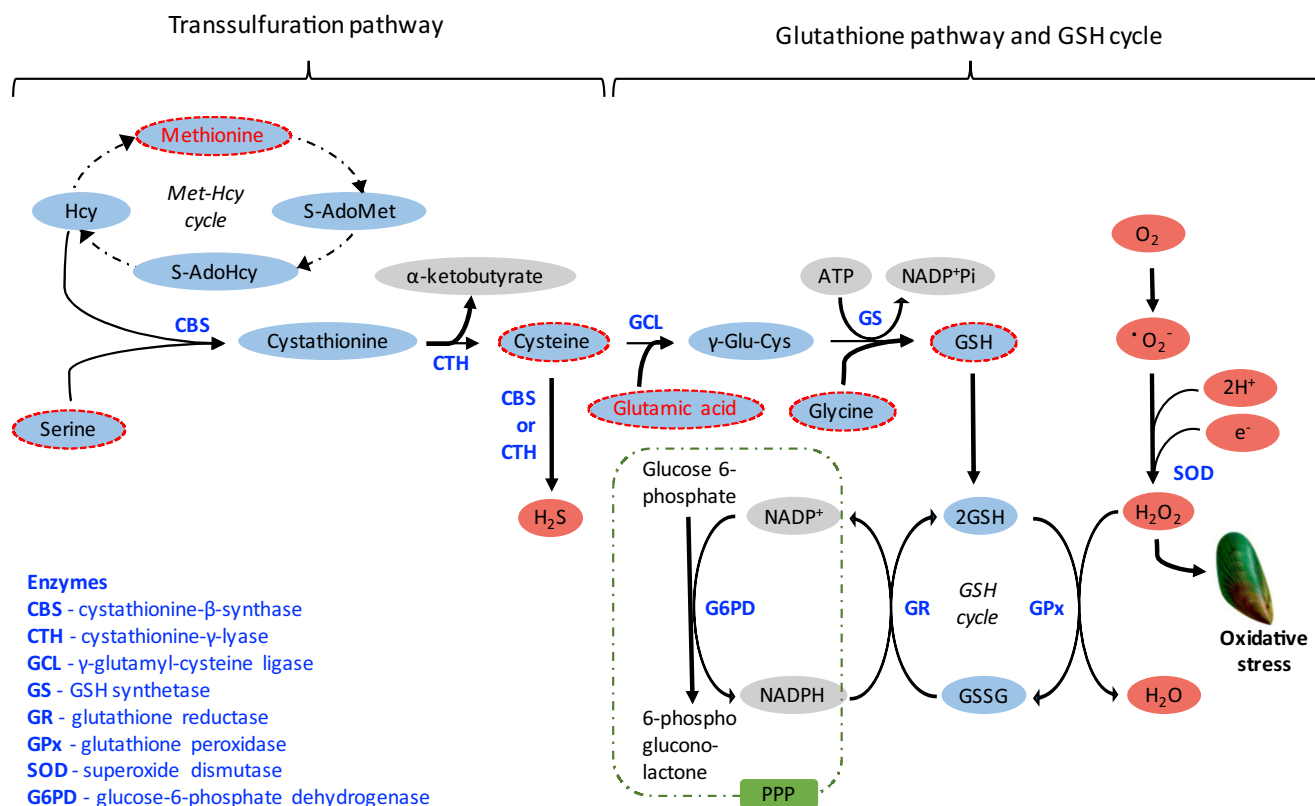

Fig. 4 Schematic representation of the relationship between transsulfuration pathway, glutathione pathway and oxidative stress. Compounds with red dash outlines are metabolites that were identified in this data set whereas compounds in red characters and red dash outlines were significantly different between control and infected mussels. Enzymes are shown in bold and blue characters. Hcy, homocysteine; S-AdoMet, S-adenosylmethionine; S-AdoHcy, S-adenosylhomocysteine; Met-Hcy cycle, Methionine-homocysteine cycle

macrophages is known to lead to massive accumulations of TCA intermediates (citric acid, succinic acid, fumaric acid and malic acid) (Jha et al. 2015). These accumulations are due to two characteristic breaking points in the TCA cycle (Jha et al. 2015; Tannahill et al. 2013). The first break occurs at isocitrate dehydrogenase (IDH), which catalyzes the oxidative decarboxylation of isocitrate into alpha-ketoglutarate. Thus, the IDH break leads to accumulation of citric acid that can act as a precursor to generate fatty acids for membrane biogenesis, prostaglandin production (Infantino et al. 2011; O'Neill et al. 2016) and itaconic acid (ITA) (Michelucci et al. 2013). In this study, we did not observe a significant increase of citric acid, but the accumulation of ITA suggests that any excess citric acid was used as its precursor during infection (Fig. 5). The second characteristic break-point of the TCA cycle occurs at the succinate dehydrogenase/respiratory complex II (SDH/CII), which can lead to an accumulation of succinic acid (reviewed by Gaber et al. 2017). As a consequence, it has been suggested that the presence of an active variant of the aspartate-arginosuccinate shunt replenishes production of fumaric acid and malic acid, which inhibits the activity of

succinate dehydrogenase (Gaber et al. 2017; Jha et al. 2015). In mussels challenged with *Vibrio* sp. DO1, we observed significantly elevated levels of succinic acid, fumaric acid and malic acid, which could be due to a similar second break-point feature of the TCA cycle in vertebrate macrophages/haemocytes. Previous studies have also reported the accumulation of ITA and succinic acid in virus-exposed oysters (Young et al. 2017). These results suggest that a similar mechanism of TCA cycle interruption may be a consequence of pathogenic infections across diverse taxa.

Inflammation

Accumulation of ROS, succinic acid and ITA in mussels exposed to *Vibrio* sp. DO1 may suggest inflammatory responses in infected mussels. Inflammation is a complex biological response of tissues to harmful stimuli (i.e. pathogens and irritants) and is considered to be a critical first line of defense of both vertebrates and invertebrates (Rowley 1996). Inflammation also is a protective mechanism involving humoral and cell mediators of the immune system. In
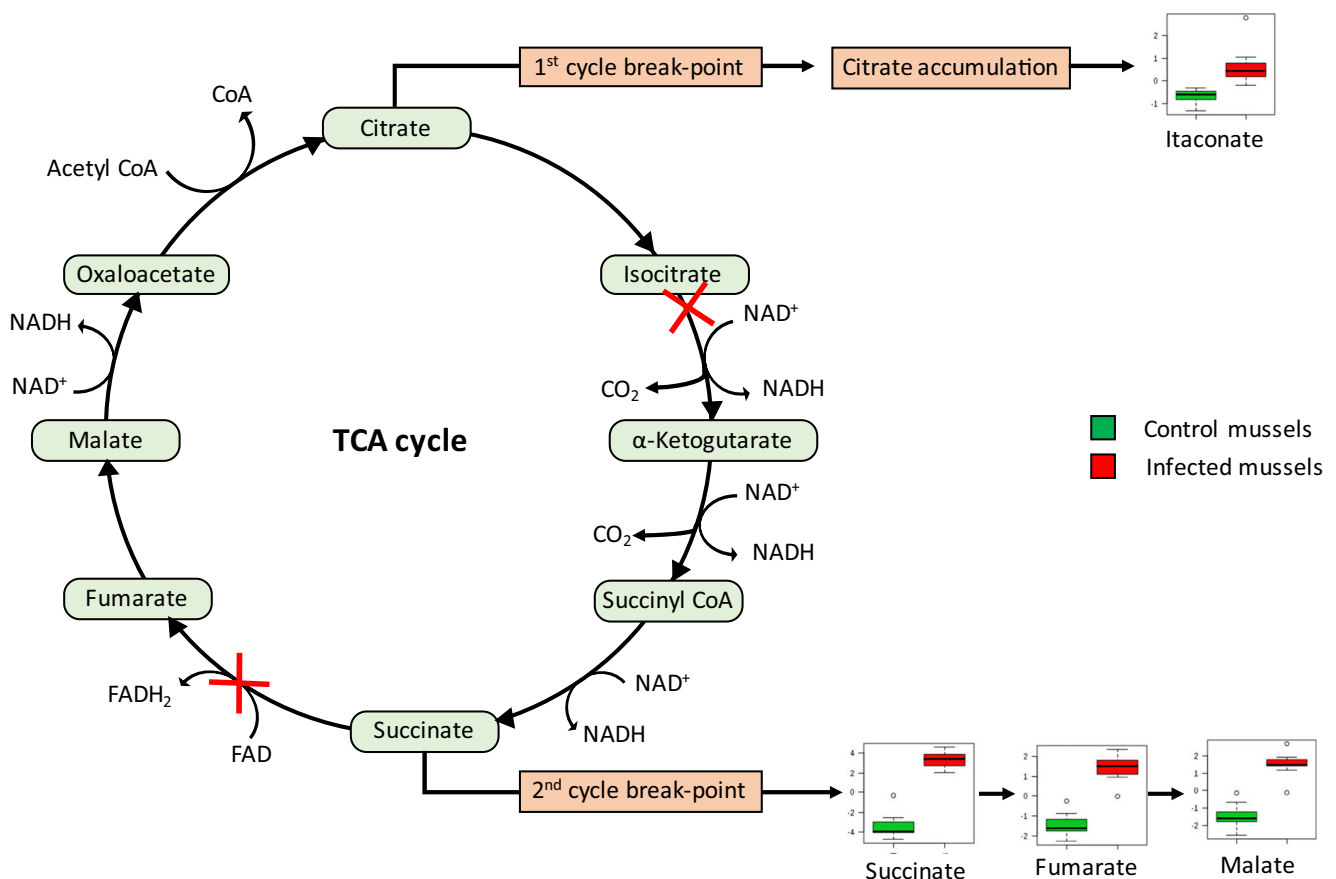

Fig. 5 Two TCA cycle break-points in *V. coralliilyticus*-infected mussels. The first break was after citrate, resulting in accumulation of citrate, which was used to generate itaconate in mussel haemolymph. The second characteristic break-point of TCA cycle occurred at succinate dehydrogenase/respiratory complex II (SDH/CII) that leads to the accumulation of succinate. Elevated levels of succinate replenish production of fumarate and malate. Box plots of metabolites are based on *t* test analysis, showing relative abundances of metabolites in control (green) and infected (red) mussels

mammalians, well-described molecular mediators are cytokines, prostaglandins, NO and ROS produced by both innate and adaptive immune cells (Mills and O'Neill 2014). Numerous studies on the biology and pathology of molluscs over the last decades has predominantly revealed that the inflammatory response in molluscs may be driven by a pool of functionally conserved molecules, such as those observed in vertebrates (De Vico and Carella 2012; Humphries and Yoshino 2003; Ottaviani et al. 2010; Rowley 1996).

ROS are signaling molecules and mediators that play a central role in the progression of inflammatory responses (Mittal et al. 2014). An increase in ROS, which leads to acute inflammation, has been well described in many studies (Fubini and Hubbard 2003; Mittal et al. 2014; Zhou et al. 2010). Hence, the increase of ROS production observed in infected mussels in this study may also trigger inflammation.

Succinic acid is known as a metabolic signal in inflammation (Mills and O'Neill 2014; Tannahill et al. 2013). In mammalians, succinic acid directly stabilizes the transcription factor hypoxia-inducible factor-1α (HIF-1α) (Mills and O'Neill 2014; Tannahill et al. 2013) or indirectly stabilizes HIF-1α by accumulation of mitochondrial ROS levels via oxidation of succinic acid to form fumaric acid by succinate dehydrogenase (SDH) (Mills et al. 2016). Once stabilized, HIF-1α activates target genes that support the inflammation (Mills et al. 2016; Tannahill 2013). In marine bivalves, the critical role of HIF-α in regulation of respiratory burst activity of the Pacific oyster (Crassostrea gigas) hemocytes has been demonstrated (Choi et al. 2013). Thus, accumulation of succinic acid in Vibrio-exposed mussels may play an important role in inflammatory responses of these mussels in this study.

ITA is a highly induced metabolite during macrophage activation, and it presently has been recognized as a major physiological regulator of inflammation (Lampropoulou et al. 2016). Lampropoulou et al. (2016) investigated the role of ITA in LPS-activated macrophages and found that ITA regulates succinic acid levels, mitochondrial respiration and ROS production. Similarly, we observed a significant increase in ITA, succinic acid and ROS production in mussels exposed to Vibrio sp. DO1. This suggests that a similar critical role of ITA in inflammatory responses may exist in marine bivalves. However, further investigation is needed to confirm the involvement of ITA in regulation of succinic acid and inflammation in invertebrates.

The amino acid gamma-aminobutyric acid (GABA) is well known as an important inhibitory neurotransmitter in the central nervous system for inflammation suppression of both vertebrates and invertebrates (Eriksson and Panula 1994). Molecular cloning of GABAA receptor-associated protein (GABARAP) from abalone (Haliotis diversicolor) and its expression in different abalone tissues after bacterial challenge suggest its vital role in the innate immune system of molluscs (Bai et al. 2012). Indeed, a decrease in GABA was found in the haemolymph of Pacific oyster (Crassostrea gigas) 6 h after LPS stimulation (Li et al. 2016). Interestingly, GABA could indirectly inhibit cellular immune and humoral immune responses by reducing the production of pro-inflammatory cytokines (CgIL-17 and CgTNF) and immune effectors (CgSOD and CgBPI) (Li et al. 2016). In our case, we also observed the decrease of GABA in infected mussels, suggesting that this metabolite may have a function in suppression of the immune-mediated pro-inflammatory reactions.

Amino Acid Metabolism and Protein Synthesis

Decreases in a number of amino acids in infected mussels suggest diverse disruptions of amino acid metabolism and protein biosynthesis. For example, the branched-chain amino acids (BCAA), including leucine, isoleucine and valine, are essential metabolites for the immune system, which provide energy and act as the precursors for biosynthesis of new molecules and cells, especially lymphocytes (Calder 2006). When infection occurs, there is a high demand of BCAA for lymphocytes to synthesize protein, RNA and DNA and other immune cell functions (Calder 2006). Similarly, we observed a decrease of BCAAs in haemolymph of mussels challenged with Vibrio sp. DO1, which suggest the high demand in BCAAs for immune activities. In contrast, Liu et al. (2013a) found an increase of BCAAs in the hepatopancreas of clams exposed to V. anguillarum. These differences in results from tissue and haemolymph analyses may be due to tissue-specific responses of hosts to infections, which have been reported in several studies (Liu et al. 2014a; Lu et al. 2017). In addition to BCAAs, we found significant decreases in other amino acids, such as tryptophan and aspartic acid. Tryptophan is an essential amino acid that is required by all life forms for the regulation of protein synthesis. It is also a substrate for other major biosynthetic routes, such as the synthesis of serotonin, essential cellular factors and the kynurenine pathway (Schröcksnadel et al. 2006). Aspartic acid is an α-amino acid that is used in protein biosynthesis (Voet et al. 2016). Hence, the decrease in these important amino acids in haemolymph of infected mussels suggests an immune stimulation by Vibrio sp. DO1 infection and the disturbance of amino acid metabolism and protein biosynthesis by the pathogen.

Conclusions

We report the first evidence of metabolic profiling of the New Zealand Greenshell™ mussel (Perna canaliculus) haemolymph exposed to Vibrio sp. DO1. We found several major perturbations on the host innate immune system of mussels resulting from Vibrio sp. DO1 infection, including oxidative stress, inflammation, disruption of TCA cycle, changes in amino acid metabolism and protein synthesis. We

identified significant alteration in a number of important metabolites. Among them, succinic acid, itaconic acid and BCAAs are involved in diverse metabolic and physiologic roles and could potentially be considered as biomarkers of *Vibrio* infection in bivalves. Hence, further characterization of these metabolites would be essential for development of health biomarkers.

Compliance with Ethical Standards

Conflict of Interest The authors declare that they have no conflict of interest.

References

Alfaro AC, Young T (2016) Showcasing metabolomic applications in aquaculture: a review. Rev Aquac. https://doi.org/10.1111/raq.12152

Allam B, Raftos D (2015) Immune responses to infectious diseases in bivalves. J Invertebr Pathol 131:121–136

Anderson RS, Good RA (1976) Opsonic involvement in phagocytosis by mollusk hemocytes. J Invertebr Pathol 27:57–64

Asensi M, Sastre J, Pallardo FV, Lloret A, Lehner M, Garcia-de-la Asuncion J, Viña J (1999) [23] ratio of reduced to oxidized glutathione as indicator of oxidative stress status and DNA damage. Methods Enzymol 299:267–276

Austin B, Austin D, Sutherland R, Thompson F, Swings J (2005) Pathogenicity of vibrios to rainbow trout (Oncorhynchus mykiss, Walbaum) and Artemia nauplii. Environ Microbiol 7:1488–1495

Bachère E, Rosa RD, Schmitt P, Poirier AC, Merou N, Charrière GM, Destoumieux-Garzón D (2015) The new insights into the oyster antimicrobial defense: cellular, molecular and genetic view. Fish Shellfish Immunol 46:50–64

Bai R, You W, Chen J, Huang H, Ke C (2012) Molecular cloning and expression analysis of GABA a receptor-associated protein (GABARAP) from small abalone, Haliotis diversicolor. Fish Shellfish Immunol 33:675–682

Bassim S, Genard B, Gauthier-Clerc S, Moraga D, Tremblay R (2015) Ontogeny of bivalve immunity: assessing the potential of next-generation sequencing techniques. Rev Aquac 7:197–217

Ben-Haim Y, Thompson FL, Thompson CC, Cnockaert MC, Hoste B, Swings J, Rosenberg E (2003) Vibrio coralliilyticus sp. nov., a temperature-dependent pathogen of the coral Pocillopora damicornis. Int J Syst Evol Microbiol 53:309–315

Bindokas VP, Jordan J, Lee CC, Miller RJ (1996) Superoxide production in rat hippocampal neurons: selective imaging with hydroethidine. J Neurosci 16:1324–1336

Brown C (1981) A study of two shellfish-pathogenic Vibrio strains isolated from a Long Island hatchery during a recent outbreak of disease [New York]. J Shellfish Res 1:83–87

Buggé DM, Hégaret H, Wikfors GH, Allam B (2007) Oxidative burst in hard clam (Mercenaria mercenaria) haemocytes. Fish Shellfish Immunol 23:188–196

Calder PC (2006) Branched-chain amino acids and immunity. J Nutr 136:288S–293S

Choi SH, Jee BY, Lee SJ, Cho MY, Lee SJ, Kim JW, Jeong HD, Kim KH (2013) Effects of RNA interference-mediated knock-down of hypoxia-inducible factor-α on respiratory burst activity of the Pacific oyster Crassostrea gigas hemocytes. Fish Shellfish Immunol 35:476–479

Chouchani ET, Pell VR, Gaude E, Aksentijević D, Sundier SY, Robb EL, Logan A, Nadtochiy SM, Ord ENJ, Smith AC, Eyassu F, Shirley R, Hu CH, Dare AJ, James AM, Rogatti S, Hartley RC, Eaton S, Costa ASH, Brookes PS, Davidson SM, Duchen MR, Saeb-Parsy K, Shattock MJ, Robinson AJ, Work LM, Frezza C, Krieg T, Murphy MP (2014) Ischaemic accumulation of succinate controls reperfusion injury through mitochondrial ROS. Nature 515:431–435

Costa MM, Prado-Alvarez M, Gestal C, Li H, Roch P, Novoa B, Figueras A (2009) Functional and molecular immune response of Mediterranean mussel (Mytilus galloprovincialis) haemocytes against pathogen-associated molecular patterns and bacteria. Fish Shellfish Immunol 26:515–523

De Vico G, Carella F (2012) Morphological features of the inflammatory response in molluscs. Res Vet Sci 93:1109–1115

Dumbauld BR, Kauffman BE, Trimble AC, Ruesink JL (2011) The Willapa Bay oyster reserves in Washington state: fishery collapse, creating a sustainable replacement, and the potential for habitat conservation and restoration. J Shellfish Res 30:71–83

Elston R, Leibovitz L, Relyea D, Zatila J (1981) Diagnosis of vibriosis in a commercial oyster hatchery epizootic: diagnostic tools and management features. Aquaculture 24:53–62

Elston RA, Hasegawa H, Humphrey KL, Polyak IK, Häse CC (2008) Re-emergence of vibrio tubiashii in bivalve shellfish aquaculture: severity, environmental drivers, geographic extent and management. Dis Aquat Org 82:119–134

Eriksson KS, Panula P (1994) Gamma-aminobutyric acid in the nervous system of a planarian. J Comp Neurol 345:528–536

Espinosa-Diez C, Miguel V, Mennerich D, Kietzmann T, Sánchez-Pérez P, Cadenas S, Lamas S (2015) Antioxidant responses and cellular adjustments to oxidative stress. Redox Biol 6:183–197

Estes RM, Friedman CS, Elston RA, Herwig RP (2004) Pathogenicity testing of shellfish hatchery bacterial isolates on Pacific oyster Crassostrea gigas larvae. Dis Aquat Org 58:223–230

Fleury E, Huvet A, Lelong C, de Lorgeril J, Boulo V, Gueguen Y, Bachère E, Tanguy A, Moraga D, Fabioux C, Lindeque P, Shaw J, Reinhardt R, Prunet P, Davey G, Lapègue S, Sauvage C, Corporeau C, Moal J, Gavory F, Wincker P, Moreews F, Klopp C, Mathieu M, Boudry P, Favrel P (2009) Generation and analysis of a 29,745 unique expressed sequence tags from the Pacific oyster (Crassostrea gigas) assembled into a publicly accessible database: the GigasDatabase. BMC Genomics 10:341

Fubini B, Hubbard A (2003) Reactive oxygen species (ROS) and reactive nitrogen species (RNS) generation by silica in inflammation and fibrosis. Free Radic Biol Med 34:1507–1516

Gaber T, Strehl C, Buttgereit F (2017) Metabolic regulation of inflammation. Nat Rev Rheumatol 13:267–279

Genard B, Miner P, Nicolas J-L, Moraga D, Boudry P, Pernet F, Tremblay R (2013) Integrative study of physiological changes associated with bacterial infection in Pacific oyster larvae. PLoS One 8:e64534

Goedken M, De Guise S (2004) Flow cytometry as a tool to quantify oyster defence mechanisms. Fish Shellfish Immunol 16:539–552

Gómez-Chiarri M, Guo X, Tanguy A, He Y, Proestou D (2015) The use of -omic tools in the study of disease processes in marine bivalve mollusks. J Invertebr Pathol 131:137–154

Grandiosa R, Mérien F, Pillay K, Alfaro A (2016) Innovative application of classic and newer techniques for the characterization of haemocytes in the New Zealand black-footed abalone (Haliotis iris). Fish Shellfish Immunol 48:175–184

Guo X, Ford SE (2016) Infectious diseases of marine molluscs and host responses as revealed by genomic tools. Philos Trans R Soc B 371:1–16

Gurer-Orhan H, Sabır HU, Özgüneş H (2004) Correlation between clinical indicators of lead poisoning and oxidative stress parameters in controls and lead-exposed workers. Toxicology 195:147–154

Hasanuzzaman AFM, Robledo D, Gómez-Tato A, Alvarez Dios JA, Harrison PW, Cao A, Fernández-Boo S, Villalba A, Pardo BG, Martínez P (2017) Transcriptomic profile of manila clam (Ruditapes philippinarum) haemocytes in response to Perkinsus olseni infection. Aquaculture 467:170–181

Humphries JE, Yoshino TP (2003) Cellular receptors and signal transduction in molluscan hemocytes: connections with the innate immune system of vertebrates. Integr Comp Biol 43:305–312

Infantino V, Convertini P, Cucci L, Panaro MA, di Noia MA, Calvello R, Palmieri F, Iacobazzi V (2011) The mitochondrial citrate carrier: a new player in inflammation. Biochem J 438:433–436

Jabs T (1999) Reactive oxygen intermediates as mediators of programmed cell death in plants and animals. Biochem Pharmacol 57:231–245

Jha AK, Huang SCC, Sergushichev A, Lampropoulou V, Ivanova Y, Loginicheva E, Chmielewski K, Stewart KM, Ashall J, Everts B, Pearce EJ, Driggers EM, Artyomov MN (2015) Network integration of parallel metabolic and transcriptional data reveals metabolic modules that regulate macrophage polarization. Immunity 42:419–430

Jones DP (2002) [11] redox potential of GSH/GSSG couple: assay and biological significance. Methods Enzymol 348:93–112

Kanehisa M, Goto S (2000) KEGG: Kyoto encyclopedia of genes and genomes. Nucleic Acids Res 28:27–30

Kehlet-Delgado H, Richards GP, Häse C, Mueller RS (2017) Three draft genome sequences of vibrio coralliilyticus strains isolated from bivalve hatcheries. Genome Announc 5:e01162–e01117

Kesarcodi-Watson A, Kaspar H, Lategan MJ, Gibson L (2009a) Two pathogens of Greenshell™ mussel larvae, Perna canaliculus: Vibrio splendidus and a V. Coralliilyticus/neptunius-like isolate. J Fish Dis 32:499–507

Kesarcodi-Watson A, Kaspar H, Lategan MJ, Gibson LF (2009b) Challenge of New Zealand Greenshell (TM) mussel Perna canaliculus larvae using two vibrio pathogens: a hatchery study. Dis Aquat Org 86:15–20

Kesarcodi-Watson A, Miner P, Nicolas J-L, Robert R (2012) Protective effect of four potential probiotics against pathogen-challenge of the larvae of three bivalves: Pacific oyster (Crassostrea gigas), flat oyster (Ostrea edulis) and scallop (Pecten maximus). Aquaculture 344–349:29–34

Lambert C, Soudant P, Choquet G, Paillard C (2003) Measurement of Crassostrea gigas hemocyte oxidative metabolism by flow cytometry and the inhibiting capacity of pathogenic vibrios. Fish Shellfish Immunol 15:225–240

Lampropoulou V, Sergushichev A, Bambouskova M, Nair S, Vincent EE, Loginicheva E, Cervantes-Barragan L, Ma X, Huang SCC, Griss T, Weinheimer CJ, Khader S, Randolph GJ, Pearce EJ, Jones RG, Diwan A, Diamond MS, Artyomov MN (2016) Itaconate links inhibition of succinate dehydrogenase with macrophage metabolic remodeling and regulation of inflammation. Cell Metab 24:158–166

Li E, Li C (2014) Use of RNA-seq in aquaculture research. Poult Fish Wildl Sci 2:108–109

Li M, Qiu L, Wang L, Wang W, Xin L, Li Y, Liu Z, Song L (2016) The inhibitory role of γ-aminobutyric acid (GABA) on immunomodulation of Pacific oyster Crassostrea gigas. Fish Shellfish Immunol 52:16–22

Liu X, Ji C, Zhao J, Wu H (2013a) Differential metabolic responses of clam Ruditapes philippinarum to vibrio anguillarum and Vibrio splendidus challenges. Fish Shellfish Immunol 35:2001–2007

Liu X, Zhao J, Wu H, Wang Q (2013b) Metabolomic analysis revealed the differential responses in two pedigrees of clam Ruditapes philippinarum towards Vibrio harveyi challenge. Fish Shellfish Immunol 35:1969–1975

Liu X, Ji C, Zhao J, Wang Q, Li F, Wu H (2014a) Metabolic profiling of the tissue-specific responses in mussel Mytilus galloprovincialis towards Vibrio harveyi challenge. Fish Shellfish Immunol 39:372–377

Liu X, Sun H, Wang Y, Ma M, Zhang Y (2014b) Gender-specific metabolic responses in hepatopancreas of mussel Mytilus galloprovincialis challenged by Vibrio harveyi. Fish Shellfish Immunol 40:407–413

Lu J, Shi Y, Cai S, Feng J (2017) Metabolic responses of Haliotis diversicolor to Vibrio parahaemolyticus infection. Fish Shellfish Immunol 60:265–274

McBean GJ (2012) The transsulfuration pathway: a source of cysteine for glutathione in astrocytes. Amino Acids 42:199–205

Michelucci A, Cordes T, Ghelfi J, Pailot A, Reiling N, Goldmann O, Binz T, Wegner A, Tallam A, Rausell A, Buttini M, Linster CL, Medina E, Balling R, Hiller K (2013) Immune-responsive gene 1 protein links metabolism to immunity by catalyzing itaconic acid production. Proc Natl Acad Sci 110:7820–7825

Milan M, Coppe A, Reinhardt R, Cancela LM, Leite RB, Saavedra C, Ciofi C, Chelazzi G, Patarnello T, Bortoluzzi S, Bargelloni L (2011) Transcriptome sequencing and microarray development for the manila clam, Ruditapes philippinarum: genomic tools for environmental monitoring. BMC Genomics 12:234

Mills E, O'Neill LA (2014) Succinate: a metabolic signal in inflammation. Trends Cell Biol 24:313–320

Mills EL et al (2016) Succinate dehydrogenase supports metabolic repurposing of mitochondria to drive inflammatory macrophages. Cell 167:457–470.e413

Mittal M, Siddiqui MR, Tran K, Reddy SP, Malik AB (2014) Reactive oxygen species in inflammation and tissue injury. Antioxid Redox Signal 20:1126–1167

Moreira R, Balseiro P, Planas JV, Fuste B, Beltran S, Novoa B, Figueras A (2012) Transcriptomics of in vitro immune-stimulated hemocytes from the manila clam Ruditapes philippinarum using high-throughput sequencing. PLoS One 7:e35009

Moreira R, Milan M, Balseiro P, Romero A, Babbucci M, Figueras A, Bargelloni L, Novoa B (2014) Gene expression profile analysis of manila clam (Ruditapes philippinarum) hemocytes after a vibrio alginolyticus challenge using an immune-enriched oligo-microarray. BMC Genomics 15:267

Nikiforova VJ, Willmitzer L (2007) Network visualization and network analysis. In: Baginsky S, Fernie AR (eds) Plant systems biology. Birkhäuser Basel, Basel, pp 245–275

O'Neill LAJ, Kishton RJ, Rathmell J (2016) A guide to immunometabolism for immunologists. Nat Rev Immunol 16:553–565

Ottaviani E, Franchini A, Malagoli D (2010) Inflammatory response in molluscs: cross-taxa and evolutionary considerations. Curr Pharm Des 16:4160–4165

Pauletto M, Milan M, Moreira R, Novoa B, Figueras A, Babbucci M, Patarnello T, Bargelloni L (2014) Deep transcriptome sequencing of Pecten maximus hemocytes: a genomic resource for bivalve immunology. Fish Shellfish Immunol 37:154–165

Philipp EE et al (2012) Massively parallel RNA sequencing identifies a complex immune gene repertoire in the lophotrochozoan Mytilus edulis. PLoS One 7:e33091

Plumb JA, Hanson LA (2011) Health maintenance and principal microbial diseases of cultured fishes. Wiley, New York

Richards GP, Bono JL, Watson MA, Needleman DS (2014) Complete genome sequence for the shellfish pathogen vibrio coralliilyticus RE98 isolated from a shellfish hatchery. Genome Announc 2: e01253–e01214

Richards GP, Watson MA, Needleman DS, Church KM, Häse CC (2015) Mortalities of eastern and Pacific oyster larvae caused by the pathogens vibrio coralliilyticus and vibrio tubiashii. Appl Environ Microbiol 81:292–297

Rosa RD, De Lorgeril J, Tailliez P, Bruno R, Piquemal D, Bachère E (2012) A hemocyte gene expression signature correlated with predictive capacity of oysters to survive vibrio infections. BMC Genomics 13:252

Rowley AF (1996) The evolution of inflammatory mediators. Mediat Inflamm 5:3–13

Rozenblat YB-H, Rosenberg E (2004) Temperature-regulated bleaching and tissue lysis of Pocillopora damicornis by the novel pathogen vibrio coralliilyticus. In: Rosenberg E, Loya Y (eds) Coral health and disease. Springer, Berlin Heidelberg, pp 301–324

Sanders ER (2012) Aseptic laboratory techniques: plating methods. J Vis Exp 63:3064

Schröcksnadel K, Wirleitner B, Winkler C, Fuchs D (2006) Monitoring tryptophan metabolism in chronic immune activation. Clin Chim Acta 364:82–90

Seol HS, Lee SE, Song JS, Lee HY, Park S, Kim I, Singh SR, Chang S, Jang SJ (2016) Glutamate release inhibitor, Riluzole, inhibited proliferation of human hepatocellular carcinoma cells by elevated ROS production. Cancer Lett 382:157–165

Smart KF, Aggio RBM, Van Houtte JR, Villas-Boas SG (2010) Analytical platform for metabolome analysis of microbial cells using methyl chloroformate derivatization followed by gas chromatography-mass spectrometry. Nat Protoc 5:1709–1729

Smith MT, Vermeulen R, Li G, Zhang L, Lan Q, Hubbard AE, Forrest MS, McHale C, Zhao X, Gunn L, Shen M, Rappaport SM, Yin S, Chanock S, Rothman N (2005) Use of 'Omic' technologies to study humans exposed to benzene. Chem Biol Interact 153–154:123–127

Song L, Wang L, Qiu L, Zhang H (2010) Bivalve Immunity. In: Söderhäll K (ed) Invertebrate immunity. Springer US, Boston, pp 44–65

Sun Y, Zhang Y, Fu X, Zhang R, Zou J, Wang S, Hu X, Zhang L, Bao Z (2014) Identification of two secreted ferritin subunits involved in immune defense of yesso scallop Patinopecten yessoensis. Fish Shellfish Immunol 37:53–59

Tannahill G et al (2013) Succinate is an inflammatory signal that induces IL-1 [bgr] through HIF-1 [agr]. Nature 496:238–242

Torreilles J, Guérin M-C, Roch P (1996) Reactive oxygen species and defense mechanisms in marine bivalves. C R Acad Sci III 319:209–218

Travers M-A, Boettcher Miller K, Roque A, Friedman CS (2015) Bacterial diseases in marine bivalves. J Invertebr Pathol 131:11–31

Tretter L, Patocs A, Chinopoulos C (2016) Succinate, an intermediate in metabolism, signal transduction, ROS, hypoxia, and tumorigenesis. Biochim Biophys Acta 1857:1086–1101

Venier P, de Pittà C, Bernante F, Varotto L, de Nardi B, Bovo G, Roch P, Novoa B, Figueras A, Pallavicini A, Lanfranchi G (2009) MytiBase: a knowledgebase of mussel (M. Galloprovincialis) transcribed sequences. BMC Genomics 10:72

Villas-Bôas SG, Smart KF, Sivakumaran S, Lane GA (2011) Alkylation or Silylation for analysis of amino and non-amino organic acids by GC-MS? Meta 1:3–20

Voet D, Voet JG, Pratt CW (2016) Fundamentals of biochemistry: life at the molecular level. Wiley, New York

Xia J, Wishart DS (2010) MetPA: a web-based metabolomics tool for pathway analysis and visualization. Bioinformatics 26:2342–2344

Xia J, Sinelnikov IV, Han B, Wishart DS (2015) MetaboAnalyst 3.0—making metabolomics more meaningful. Nucleic Acids Res 43: 251–257

Young T, Alfaro AC (2016) Metabolomic strategies for aquaculture research: a primer. Rev Aquac 0:1–31

Young T, Kesarcodi-Watson A, Alfaro AC, Merien F, Nguyen TV, Mae H, le DV, Villas-Bôas S (2017) Differential expression of novel metabolic and immunological biomarkers in oysters challenged with a virulent strain of OsHV-1. Dev Comp Immunol 73:229–245

Yue F, Shi X, Zhou Z, Wang L, Wang M, Yang J, Qiu L, Song L (2013) The expression of immune-related genes during the ontogenesis of scallop Chlamys farreri and their response to bacterial challenge. Fish Shellfish Immunol 34:855–864

Zhang L, Li L, Zhu Y, Zhang G, Guo X (2014) Transcriptome analysis reveals a rich gene set related to innate immunity in the eastern oyster (Crassostrea virginica). Mar Biotechnol 16:17–33

Zhang H, Zhai Y, Yao L, Jiang Y, Li F (2017) Comparative transcriptomics reveals genes involved in metabolic and immune pathways in the digestive gland of scallop Chlamys farreri following cadmium exposure. Chin J Oceanol Limnol 35:603–612

Zhou R, Tardivel A, Thorens B, Choi I, Tschopp J (2010) Thioredoxin-interacting protein links oxidative stress to inflammasome activation. Nat Immunol 11:136–140

Zitka O et al (2012) Redox status expressed as GSH: GSSG ratio as a marker for oxidative stress in paediatric tumour patients. Oncol Lett 4:1247–1253